

ESTIMATION OF FREAK WAVE OCCURRENCE FROM DEEP TO SHALLOW WATER REGIONS

Hiroaki Kashima¹, Katsuya Hirayama¹ and Nobuhito Mori²

Nonlinear four-wave interactions amplify wave heights of deep-water generating extreme wave such as a freak wave. However, it is not clear the behavior of generated freak waves in deep-water shoaling to shallow water regions. In this study, a series of physical experiments and numerical simulations with several bathymetry configurations were conducted for unidirectional random waves from deep to shallow water regions. The maximum wave heights increase with an increase in kurtosis by third-order nonlinear interactions in deep water regions. The dependence of the kurtosis on the freak wave occurrence is weakened due to second-order nonlinear interactions associated with wave shoaling on the slope. Moreover, it is possible to understand the behavior of the high-order nonlinearity and the freak wave occurrence in shallow water regions if appropriate correction of the insufficient nonlinearity of more than $O(\epsilon^2)$ to the standard Boussinesq equation are considered analytically.

Keywords: freak wave; kurtosis, skewness; higher-order nonlinear interactions; standard Boussinesq equation

INTRODUCTION

In the past two decades, the deep-water extreme wave such as a freak wave was measured and caused several severe damages to offshore structures and vessels. An accurate estimation of maximum wave height and the prediction of the freak wave occurrence is important for marine safety and ocean development. According to several studies on freak waves in offshore, the kurtosis of the surface elevation which is indicator of the third-order nonlinear interactions (quasi-resonant four-wave interactions) can be related with a significant enhancement of freak wave occurrence (Yasuda and Mori, 1993). Janssen (2003) theoretically investigated the freak wave occurrence caused by a consequence of quasi-resonant four-wave interactions in short time. He also found that the quasi-resonant nonlinear transfer is associated with the increase of fourth-order cumulant which is equivalent to kurtosis. In addition, he introduced Benjamin-Feir Index (*BFI*) to investigate the ratio of nonlinearity to frequency dispersion for the narrow-banded unidirectional waves, given by

$$BFI = \sqrt{2} \frac{\epsilon}{\Delta} \quad (1)$$

Where ϵ is the wave steepness and Δ is the bandwidth of frequency spectrum. Furthermore, Mori and Janssen (2006) formulated the probability density function of the maximum wave height p_m by Eq. 2 and the exceedance probability of maximum wave height P_m by Eq. 3 from spectral shape through the *BFI* as an extension work of Janssen (2003), analytically.

$$p_m(H_{\max}) = \frac{N}{4} H_{\max} \exp^{\frac{-H_{\max}^2}{8}} [1 + \kappa_{40} A_H(H_{\max})] \times \exp \left\{ N \exp^{\frac{-H_{\max}^2}{8}} [1 + \kappa_{40} B_H(H_{\max})] \right\} \quad (2)$$

$$P_m(H_{\max}) = 1 - \exp \left\{ -N \exp^{\frac{-H_{\max}^2}{8}} [1 + \kappa_{40} B_H(H_{\max})] \right\} \quad (3)$$

Where

$$\kappa_{40} = \frac{\pi}{\sqrt{3}} (BFI)^2 \quad (4)$$

¹ Coastal and Ocean Engineering Field, Port and Airport Research Institute, 3-1-1 Nagase, Yokosuka, Kanagawa, 239-0826, Japan

² Maritime Disaster Research Section, Disaster Prevention Research Institute, Kyoto University, Gokasho, Uji, Kyoto, 611-0011, Japan

$$A_H(H_{\max}) = \frac{1}{384} (H_{\max}^4 - 32H_{\max}^2 + 128) \quad (5)$$

$$B_H(H_{\max}) = \frac{1}{384} H_{\max}^2 (H_{\max}^2 - 16) \quad (6)$$

where N is the number of waves for one wave train and κ_{40} is the fourth-order cumulant of the surface elevation which equals to kurtosis minus three. This framework on the estimation of freak wave, named as MJ2006 in here, was verified by the several wave flume experiments for unidirectional waves including the spatial evolution of the kurtosis, the wave height distribution and the maximum wave height distribution in detail (e.g. Mori et al., 2007; Petrova and Guedes Soares, 2009). Moreover, the recent investigation reported that directional dispersion reduces the enhancement of extreme wave generation due to the third order nonlinear interactions (Waseda et al., 2009). Mori et al. (2008, 2011) reported a new formula for the kurtosis as an extension of Eqs. 1 and 4 including the directional dispersion effects. Although the characteristics of freak wave occurrence and its prediction in deep water regions become getting clear, there are a few studies about the characteristics of freak wave propagating from deep to shallow water regions (e.g. Janssen and Onorato, 2007; Zeng and Trulsen, 2012; Trulsen et al., 2012). The most of previous studies assumed a flat bottom and quasi stationary conditions for given water depth. However, a wave transition sometimes occurs quickly from deep to shallow water regions on a steep slope. It is interesting to examine the behavior of wave group enhanced in the deep-water propagating to shallow water regions.

In General, a numerical simulation using the standard Boussinesq equation has been frequently and widely used to estimate wave transformation in shallow water regions (Hirayama, 2002). The standard Boussinesq equation shows high-level performance in the design of coast and harbor structures in Japan (e.g. Hirayama, 2013a). However, it is difficult to describe the freak wave occurrence from deep to shallow water region by the standard Boussinesq equation because it can express only up to the second-order nonlinear interactions only in shallow water regions. Thus, there is a gap of governing equation between deep and shallow water region from the extreme wave modeling point of view. It is necessary to investigate the transient behaviors of the high-order nonlinearities related to the freak wave occurrence from deep to shallow water regions.

In this study, the physical experiments in a wave tank and numerical simulations using the standard Boussinesq equation were conducted to estimate the freak wave occurrence from deep to shallow water regions. First, the experimental characteristics of the freak wave occurrence from deep to shallow water regions are investigated through the transient behaviors of the high-order nonlinearities in shallow water regions. Second, the nonlinear statistical wave properties related to freak wave occurrences by the standard Boussinesq equation are investigated through the comparison with the experimental data. Finally, the parameterization of nonlinear effects is proposed to be able to estimate the probability density function of maximum wave height as freak wave occurrences in shallow water regions using the simulated results.

OUTLINES OF PHYSICAL EXPERIMENTS AND NUMERICAL SIMULATIONS

Experimental Setup

A series of the physical experiments were conducted using a two-dimensional wave tank (0.6 m wide, 1.5 m high and 35.0 m long) at Port and Airport Research Institute in Japan. The four different bathymetries were selected to investigate the freak wave occurrence from deep to shallow water regions as shown in Fig. 1. The Type 1 is flat bathymetries, of which constant water depth is equal to 0.8 m. The characteristics of the freak wave occurrence without bottom effects in the water regions are investigated by the bathymetry Type 1. The Type 2 has a fixed impermeable 1/20 slope installed at the toe 1.56 m from the wave maker. The relationship between second-order and third-order nonlinear interactions and freak wave occurrence from deep to shallow water regions will be discussed in the measurements using the bathymetry Type 2. The Types 3 and 4 are the complex bathymetries composed of a combination of Type 1 and Type 2. The Type 3 has a fixed impermeable 1/30 slope installed with the toe 11.9 m from the wave maker and a flat ground bathymetry, of which constant water depth is equal to 0.2 m. In the Type 4, the two different slopes are installed at the toe 11.9 m from the wave maker and the water depth at the inflection point of them is equal to 0.2 m.

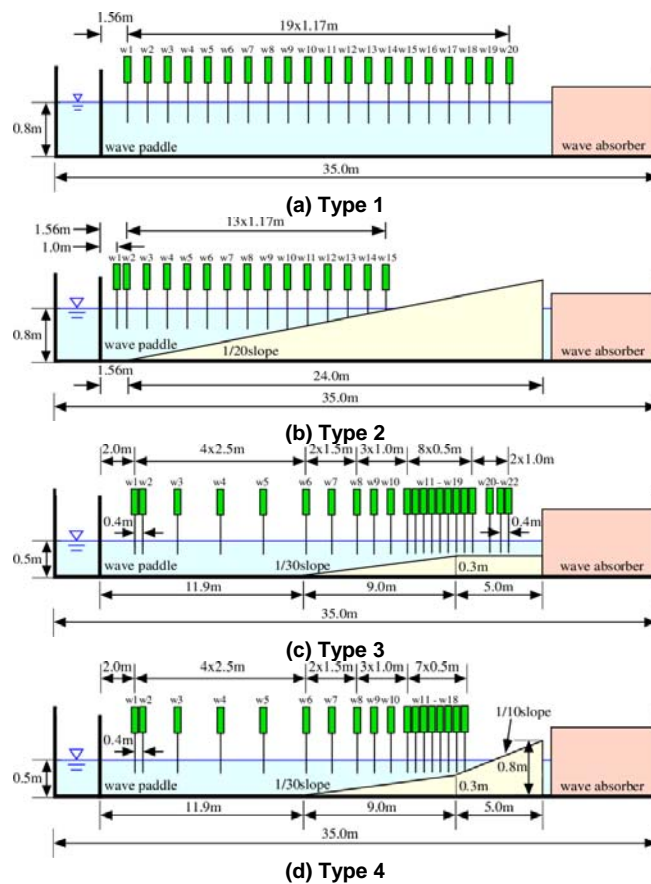


Figure 1. Cross sectional view of four different bathymetry configurations (“w” indicates location of wave gauge)

Table 1. Experimental conditions (H_i : incident wave height, h_i : water depth in front of wave maker, k_p : wave number for deep water wave with $f_p = 1.0$ Hz, L_p : wave length for deep water wave with $f_p = 1.0$ Hz, γ_i : peak enhancement factor of JONSWAP-type spectrum)

Case	H_i (cm)	h_i (m)	$k_p h_i$	H_i/L_p	γ_i	Bathymetry section
1	6.24	0.8	3.235	0.04	1.0	Type 1 and Type 2
2	6.24	0.8	3.235	0.04	3.3	Type 1 and Type 2
3	6.24	0.8	3.235	0.04	10.0	Type 1 and Type 2
4	3.12	0.8	3.235	0.02	10.0	Type 1 and Type 2
5	4.68	0.8	3.235	0.03	10.0	Type 1 and Type 2
6	6.24	0.5	2.022	0.04	10.0	Type 3 and Type 4

The six different JONSWAP-type spectra with different values of the wave steepness, H_i/L_p of 0.02, 0.03 and 0.04 and the spectral peak enhancement factor, γ_i of 1.0, 3.3 and 10.0 were performed. Here H_i is the characteristic incident wave height and L_p is the wave length for the deep water wave with the peak frequency $f_p = 1.0$ Hz, which gives the spectral peak wave number $k_p = 4.03 \text{ m}^{-1}$. The experimental conditions are summarized in Table 1.

The water surface elevation was measured by 15 to 22 capacitance-type wave gauges for each bathymetry type. An overview of the wave tank with the location of the wave gauges is shown in Fig. 1. As mentioned in the previous section, the maximum wave height depends on the number of waves in the wave train as shown in Eqs. 2 and 3. Hence the long time experiments are important to verify the effects of the number of waves for understanding the maximum wave height distribution, correctly. Therefore ten measurement sets with the different random phases for each incident wave were performed in the physical experiments. To check the sensitivity of the maximum wave height

distribution on the number of waves, the duration of each measurement was 20 minutes which corresponds to about 1,000 waves. The total number of the recorded wave height was about 10,000 waves for each case. In our analysis, the number of waves for one wave train is defined as $N = 200$. The skewness μ_3 and kurtosis μ_4 which indicate the wave nonlinearity are defined as:

$$\mu_3 = \frac{1}{\eta_{rms}^3} \frac{1}{n} \sum_{i=1}^n (\eta_i - \eta_{mn})^3 \quad (7)$$

$$\mu_4 = \frac{1}{\eta_{rms}^4} \frac{1}{n} \sum_{i=1}^n (\eta_i - \eta_{mn})^4 \quad (8)$$

where η_i is the water surface elevation, η_{mn} is the time mean value of η_i , η_{rms} is the root mean square value of η_i , and n is the number of data points. From Eqs. 7 and 8, the linear random wave corresponds $\mu_3 = 0.0$ and $\mu_4 = 3.0$.

Numerical Setup

A series of the numerical simulation, named NOWT-PARI (Nonlinear Wave Transformation model by Port and Airport Research Institute) originally developed by Hirayama (2002), were performed to estimate the freak wave occurrence in shallow water regions. These simulations are based on the standard Boussinesq equation with improved the dispersion characteristics as reported by Madsen and Sørensen (1992). The fundamental equations of continuity and momentum for x and y directions can be expressed as follows:

$$\frac{\partial \eta}{\partial t} + \frac{\partial P}{\partial x} + \frac{\partial Q}{\partial y} = 0 \quad (9)$$

$$\begin{aligned} & \frac{\partial P}{\partial t} + gD \frac{\partial \eta}{\partial x} + \epsilon \left[\frac{\partial}{\partial x} \left(\frac{P^2}{D} \right) + \frac{\partial}{\partial y} \left(\frac{PQ}{D} \right) \right] \\ & = \mu^2 \left[\left(B + \frac{1}{3} \right) h^2 \left(\frac{\partial^3 P}{\partial x^2 \partial t} + \frac{\partial^3 Q}{\partial x \partial y \partial t} \right) + Bgh^3 \left(\frac{\partial^3 \eta}{\partial x^3} + \frac{\partial^3 \eta}{\partial x \partial y^2} \right) \right. \\ & \quad \left. + h \frac{\partial h}{\partial y} \left(\frac{1}{6} \frac{\partial^2 Q}{\partial x \partial t} + Bgh \frac{\partial^2 \eta}{\partial x \partial y} \right) + h \frac{\partial h}{\partial x} \left(\frac{1}{3} \frac{\partial^2 P}{\partial x \partial t} + \frac{1}{6} \frac{\partial^2 Q}{\partial y \partial t} + 2Bgh \frac{\partial^2 \eta}{\partial x^2} + Bgh \frac{\partial^2 \eta}{\partial y^2} \right) \right] \quad (10) \end{aligned}$$

$$\begin{aligned} & \frac{\partial Q}{\partial t} + gD \frac{\partial \eta}{\partial y} + \epsilon \left[\frac{\partial}{\partial x} \left(\frac{P^2}{D} \right) + \frac{\partial}{\partial y} \left(\frac{Q^2}{D} \right) \right] \\ & = \mu^2 \left[\left(B + \frac{1}{3} \right) h^2 \left(\frac{\partial^3 P}{\partial x \partial y \partial t} + \frac{\partial^3 Q}{\partial y^2 \partial t} \right) + Bgh^3 \left(\frac{\partial^3 \eta}{\partial x^2 \partial y} + \frac{\partial^3 \eta}{\partial y^3} \right) \right. \\ & \quad \left. + h \frac{\partial h}{\partial x} \left(\frac{1}{6} \frac{\partial^2 P}{\partial y \partial t} + Bgh \frac{\partial^2 \eta}{\partial x \partial y} \right) + h \frac{\partial h}{\partial y} \left(\frac{1}{6} \frac{\partial^2 P}{\partial x \partial t} + \frac{1}{3} \frac{\partial^2 Q}{\partial y \partial t} + Bgh \frac{\partial^2 \eta}{\partial x^2} + 2Bgh \frac{\partial^2 \eta}{\partial y^2} \right) \right] \quad (11) \end{aligned}$$

where η is the instantaneous water surface elevation. P and Q are the depth-integrated velocity components (flux per unit width) in x and y directions, respectively. h is the water depth and D is the total water depth which equals to the water depth plus the instantaneous water surface elevation. g is the gravitational acceleration. ϵ and μ are the small parameters normalized by wave number k , which indicate the nonlinear effects (H/h) and dispersion effects (kh), respectively, where H is the wave height. The governing equations take into account up to $O(\epsilon)$ for nonlinearity and $O(\mu^2)$ for dispersion. The parameter B is the dispersion enhancement coefficient. For $B = 1/15$, the weak-nonlinear wave shoaling and wave dispersion closely correspond to the linear wave theory (Madsen and Sørensen, 1992). The further improvements of NOWT-PARI (*e.g.* wave breaking, run up and wave overtopping models) have been conducted to accurately estimate the wave transformation for engineering application in coastal and harbor zones (*e.g.* Hirayama, 2013b).

The governing equations is discretized by the ADI (Alternating Direction Implicit) method with the staggered grid, and the second-order central difference method and the Euler explicit method are applied to the spatial and temporal derivative terms, respectively. In the numerical simulations, we will consider the only most particular case (*i.e.*, the strongest nonlinear case), which corresponds to a

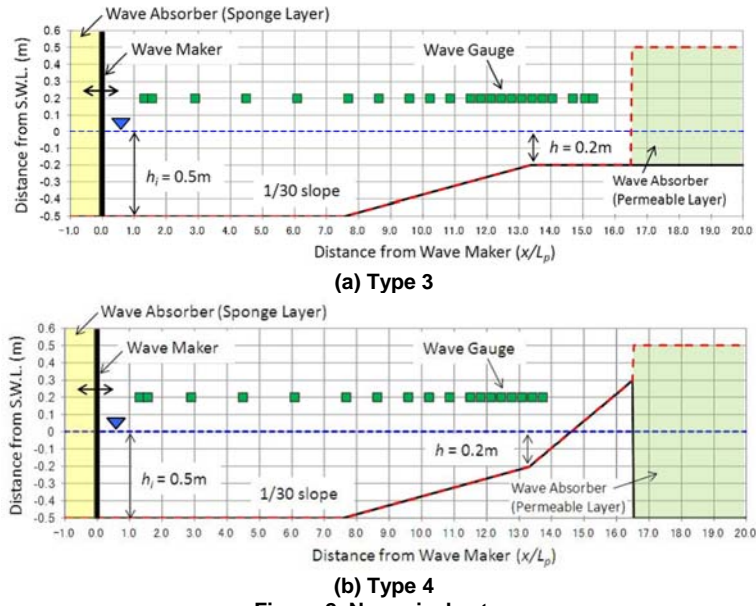


Figure 2. Numerical setup

JONSWAP-type spectrum with $\gamma_i = 10.0$ and wave steepness, H_i/L_p of 0.04 for the bathymetry Type 3 and Type 4. The numerical domains for two bathymetry types were setup as shown in Fig. 2. The wave signal was generated at the leftward boundary and propagated in the right side direction in the numerical domains, and the water depth in front of the wave maker h_i was 0.5 m. The sponge layer $1.0 \cdot L_p$ long was installed at the leftward boundary corresponding to the wave maker and the permeable layer 5.5 m long was installed at the rightward boundary corresponding to the wave absorber. The computational spatial and temporal resolutions were setup $dx = 0.05$ m and $dt = 0.001$ s to get high accuracy results of the numerical simulations, respectively.

RESULTS AND DISCUSSION

Characteristics of freak wave occurrence in deep water regions

The characteristics of the freak wave occurrence in deep water regions were investigated through the comparison with MJ2006. Fig. 3 shows the spatial developments of both skewness and kurtosis of the surface elevation for the experimental data in deep water regions. The horizontal axis is the dimensionless distance from the wave maker x/L_p and the vertical axes are the skewness and kurtosis which are given as the average values of 50 wave trains, respectively. The marks are the experimental data for Case 1 to 5, respectively. As can be noticed, the distributions of both skewness and kurtosis deviate from Rayleigh distribution for which the values of the skewness and kurtosis are equal to 0.0 and 3.0. The skewness of the experimental data is relatively constant with the values according to the incident wave steepness without relying on the distance from the wave maker. For the cases of $H_i/L_p = 0.02, 0.03$ and 0.04 , the spatial averaged values of the skewness are 0.06, 0.11 and 0.18, respectively. The skewness is analytically represented by the second-order nonlinear interactions of Longuet-Higgins (1963) and is simply given for deep-water random waves as

$$\mu_3^{(2)} = 3k_p \sqrt{m_0} \quad (12)$$

where m_0 indicates the characteristic wave height from the wave energy. Thus the skewness depends on the wave steepness for the second-order nonlinearity. The theoretical values of the skewness $\mu_3^{(2)}$ are 0.09, 0.12 and 0.16 for each wave steepness $H_i/L_p = 0.02, 0.03$ and 0.04 , respectively. Therefore the experimental results show a good agreement with the development of the skewness by the second-order nonlinear interactions. On the other hand, the kurtosis for the Case 3 is monotonically increased up to 3.4 as the wave propagates. The kurtosis is represented by the second-order nonlinear interactions (Longuet-Higgins, 1963; Mori and Janssen, 2006) and is given by

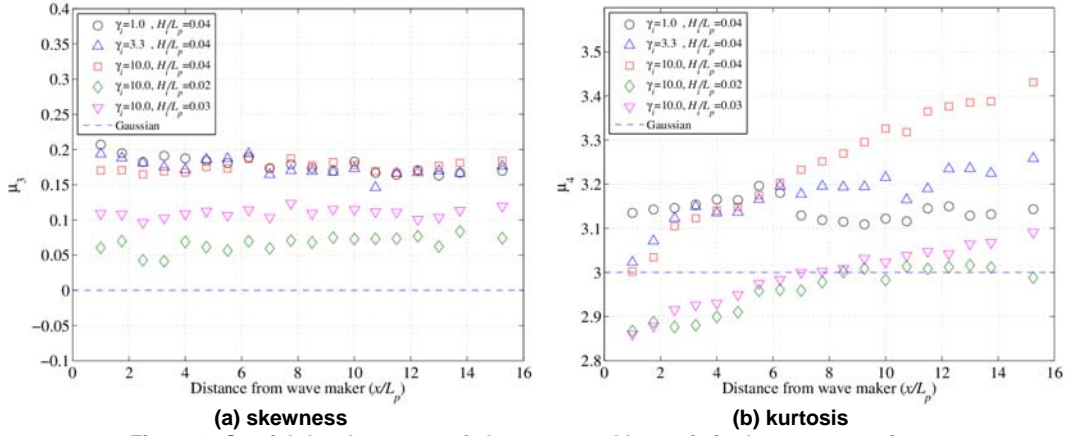


Figure 3. Spatial developments of skewness and kurtosis in deep water regions

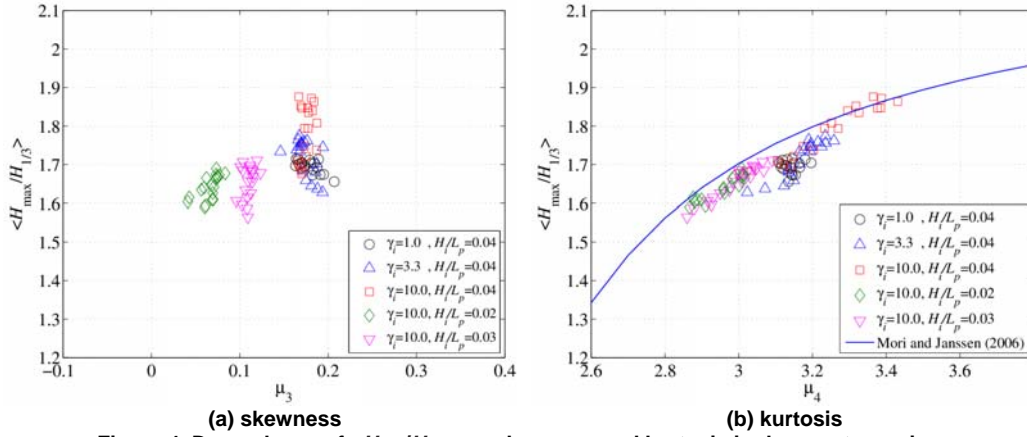


Figure 4. Dependence of $\langle H_{\max}/H_{1/3} \rangle$ on skewness and kurtosis in deep water regions

$$\mu_4^{(2)} = 3 + 24k_p^2 m_0 \quad (13)$$

The kurtosis given by the second-order nonlinear interactions $\mu_4^{(2)}$ are 3.02 to 3.04 for any wave conditions. Thus the kurtosis increase is independent of the second-order nonlinear interactions in deep water regions. These results imply that the kurtosis may be increased by the third-order nonlinear interactions under the effects of the quasi-resonant four-wave interactions in deep water regions as discussed by Mori and Yasuda (2001).

To evaluate the effects of the nonlinearity related to the freak wave occurrence on the maximum wave height in deep water regions, Fig. 4 shows the relationships between the expected value of maximum wave height $\langle H_{\max}/H_{1/3} \rangle$, and skewness and kurtosis for the deep water waves. The bracket $\langle \rangle$ indicates the ensemble-averaged value and the solid line indicates MJ2006. In Fig. 4, the experimental data show a clear dependence of the kurtosis on $\langle H_{\max}/H_{1/3} \rangle$, although $\langle H_{\max}/H_{1/3} \rangle$ is independent of the skewness because the kurtosis directly effects on the appearance of the maximum wave height as third-order nonlinear correction of the wave height. The experimental data are in good agreements with the results of MJ2006.

Characteristics of freak wave occurrence from deep to shallow water regions

In the previous section, we have investigated the freak wave occurrence in deep water regions. However, its characteristics in shallow water regions differ from that of in deep water regions because of the bottom bathymetry effects. In this section, it is examined the effects of water depth on freak wave occurrence. The wave propagation process from offshore to near shore on a fixed impermeable constant slope was setup for the bathymetry Type 2. Here we will consider the strongest nonlinear case, which corresponds to a JONSWAP-type spectrum with $\gamma_i = 10.0$, the significant wave height of 6.24 cm and the wave steepness of 0.04, initially.

Fig. 5 shows the effects of the water depth on the spatial developments of skewness and kurtosis

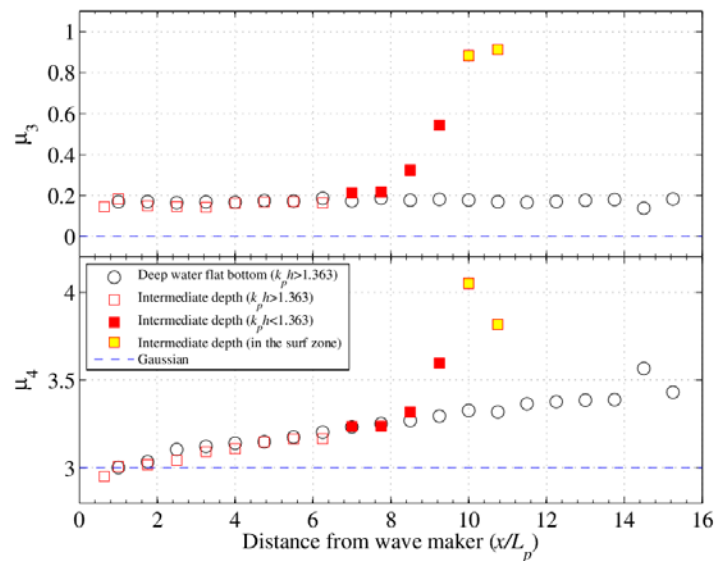


Figure 5. Effects of water depth on spatial developments of skewness and kurtosis (Incident wave condition; $\gamma = 10$, $H_i = 6.24$ cm, $H/L_p = 0.04$)

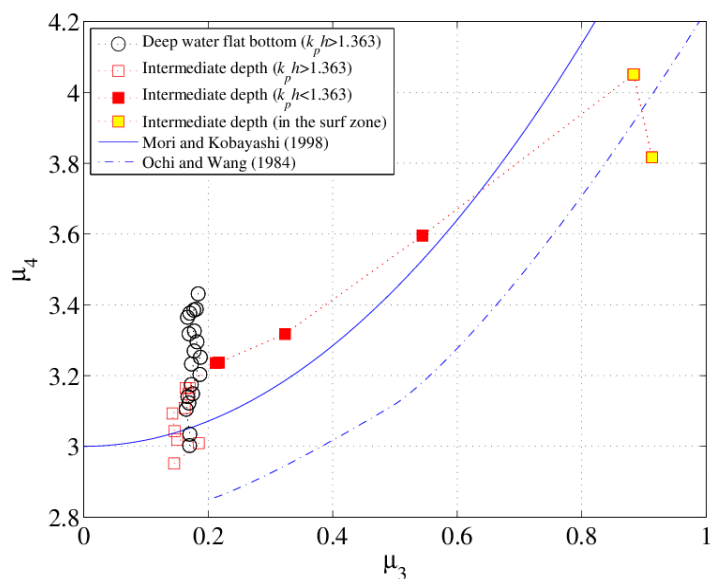


Figure 6. Relationship between skewness and kurtosis from deep to shallow water regions (Incident wave condition; $\gamma = 10$, $H_i = 6.24$ cm, $H/L_p = 0.04$)

for the strongest nonlinear case. The filled and opened marks are the experimental data of $k_p h < 1.363$ and $k_p h > 1.363$, respectively and the threshold value of $k_p h = 1.363$ corresponds to the critical condition for Benjamin-Feir instability. The yellow filled marks are the data in the surf zone. In the wave propagation process from offshore to near shore, both skewness and kurtosis have an interesting behavior at $k_p h = 1.363$ which corresponds to $x/L_p = 6.90$. In the deep water regions of $k_p h > 1.363$, the skewness is nearly-constant, $\mu_3 = 0.18$, without relying on the distance from the wave maker and the kurtosis is increased as the waves propagate. These results are similar to the development process in deep water regions of $k_p h = 3.235$ as shown in Fig. 3. However, when $k_p h$ becomes smaller than 1.363, both skewness and kurtosis are increased rapidly. In particular, the value of skewness is increased up to 1.0 on the slope, remarkably. The skewness change on the slope of $k_p h < 1.363$ is caused by the second-order nonlinear interactions associated with wave shoaling as follows.

In order to check the behavior of the nonlinearity from deep to shallow water regions, Fig. 6 shows the relationship between skewness and kurtosis for Type 1 and Type 2. The horizontal and vertical axes are skewness and kurtosis, respectively. The solid line is the second-order nonlinear

theory in consideration of the water depth change by Mori and Kobayashi (1998) and the dashed line is the empirical equation introduced by the data observed in the beach with 1.4 to 24.4 m water depth (Ochi and Wang, 1984). The theoretical and empirical equations mean that the skewness developed by the second-order nonlinear interactions associated with wave shoaling effects on the kurtosis change when the behaviors of the skewness and kurtosis obey these second-order relations. For the data of $k_p h > 1.363$, the kurtosis is independent of the skewness and is widely distributed between 2.9 and 3.6. However, the kurtosis is basically dependent on the skewness change and is increased with increase of the skewness for the data of $k_p h < 1.363$. The behaviors of the kurtosis and skewness of $k_p h < 1.363$ are similar to the two relational expressions by Mori and Kobayashi (1998) and Ochi and Wang (1984). Yuen and Lake (1982) and Janssen and Onorato (2007) reported that the energy transfer and modulation of quasi-monochromatic waves by third-order nonlinear interactions is diminished when $k_p h$ becomes smaller than 1.363. These results follow the discussion by Yuen and Lake (1982) and show that the threshold value of $k_p h = 1.363$ plays a significant role for understanding the freak wave occurrence in shallow water regions. Thus the above discussion can be summarized as follows. The kurtosis on the slope is increased by two different mechanisms. First, the kurtosis is increased by the third-order nonlinear interactions under the effects of quasi-resonant four-wave interactions until intermediate water depth of $k_p h = 1.363$, although the effects becomes weaker from offshore to near shore. After passing $k_p h = 1.363$, the shallow water effects which correspond to the second-order nonlinearities become dominant and the kurtosis is increased with the increase of the skewness given by Eqs. 12 and 13. Moreover, the development of the third-order nonlinear interactions in deep water regions of $k_p h > 1.363$ remains even in shallow water regions of $k_p h < 1.363$. This aftereffect makes the difference of the frequency distribution of the maximum wave height in shallow water regions. Finally, the kurtosis is rapidly decreased by wave breaking in the surf zone.

As mentioned above, the relationships between the nonlinear interactions and the shallow water were discussed. Here we will discuss the characteristics of the freak wave occurrence in the shallow water regions in terms of $k_p h$. To investigate the relationships between the skewness and kurtosis under the water depth change, Fig. 7 shows the dependence of the kurtosis on skewness in the shallow water regions on a slope (Type 2). The notification is same to Fig. 6 and the marks are the experimental data for Case 1 to 5, respectively. As already discussed above, the kurtosis of $k_p h < 1.363$ are basically dependent on the skewness change and they roughly obey the relations by Mori and Kobayashi (1998) and Ochi and Wang (1984) regardless of the incident wave conditions. For the data of $k_p h > 1.363$, although the value of the skewness after the waves generate is different according to the incident wave steepness (see Fig. 7 (a)), the kurtosis is distributed for the skewness independently.

We show the relationships between the expected value of maximum wave height $\langle H_{\max}/H_{1/3} \rangle$ and skewness and kurtosis from deep to shallow water regions in Fig. 8 and Fig. 9. The notifications are same to Fig. 4 and the marks are the experimental data for Case 1 to 5, respectively. The yellow filled marks are the data in the surf zone. The experimental data of $k_p h > 1.363$ show there is a clear correlation between $\langle H_{\max}/H_{1/3} \rangle$ and kurtosis although there is no systematic relation between $\langle H_{\max}/H_{1/3} \rangle$ and skewness. The MJ2006 follows the experimental data approximately. On the other hand, $\langle H_{\max}/H_{1/3} \rangle$ in the range of $k_p h < 1.363$ becomes nearly flat between 1.6 and 1.8 according to the

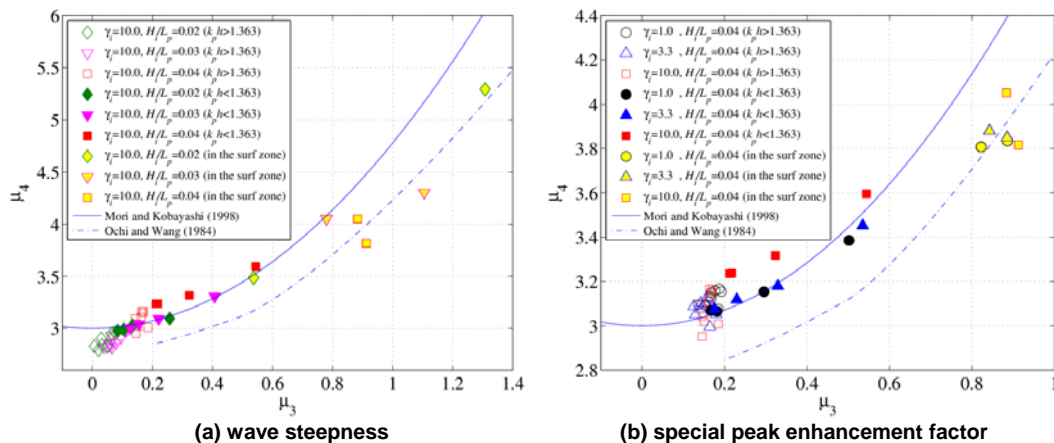


Figure 7. Relationship between skewness and kurtosis shoring from offshore to near shore

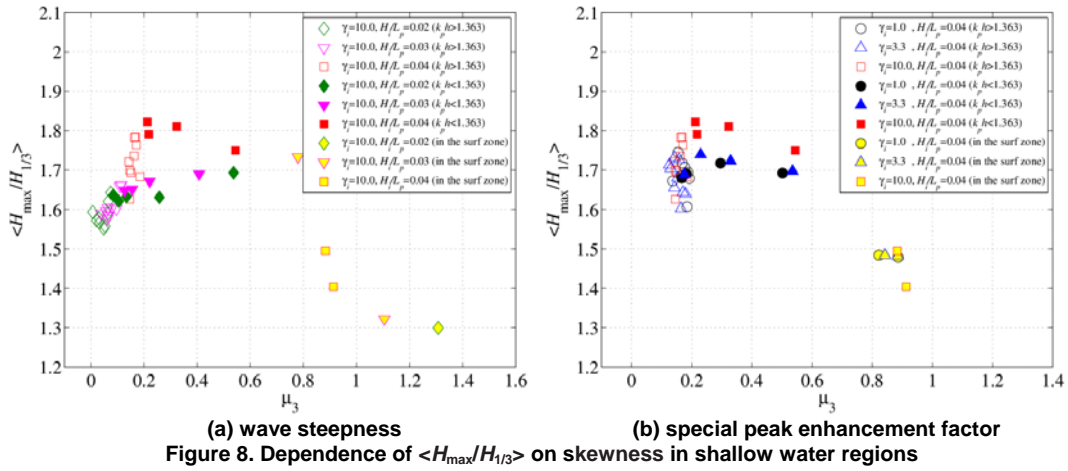


Figure 8. Dependence of $\langle H_{\max}/H_{1/3} \rangle$ on skewness in shallow water regions

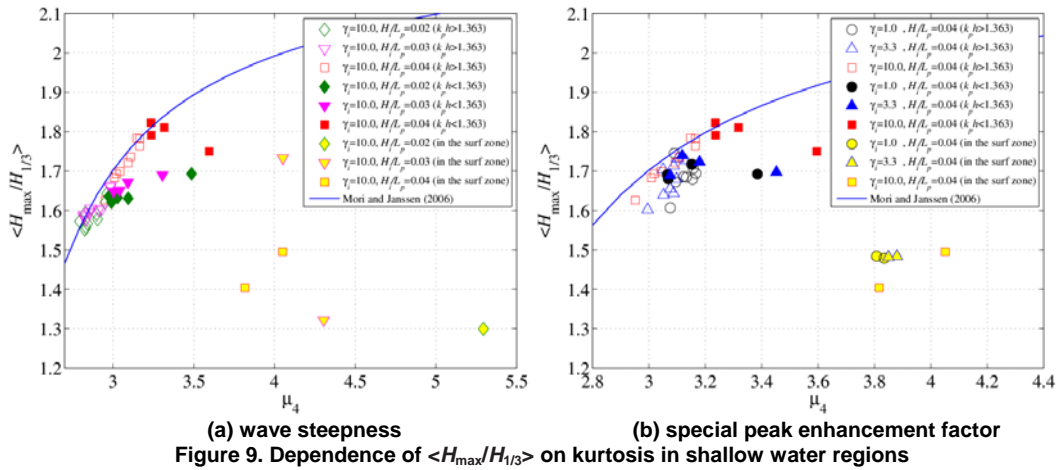


Figure 9. Dependence of $\langle H_{\max}/H_{1/3} \rangle$ on kurtosis in shallow water regions

incident wave steepness, although the skewness and kurtosis are rapidly increased under the effects of the second-order nonlinear interactions related to the shallow water effects. The dependence of $\langle H_{\max}/H_{1/3} \rangle$ on kurtosis becomes weakened in shallow water regions. After that, the values of $\langle H_{\max}/H_{1/3} \rangle$ in the surf zone are rapidly decreased by the shallow water wave breaking. Concluding above discussion, it is possible to estimate the behavior of $\langle H_{\max}/H_{1/3} \rangle$ by using the threshold value of $k_p h = 1.363$ in the shallow water regions. Therefore, the changes of wave height distribution can be expressed as a function of kurtosis from deep to shallow water regions as a proxy of the second-order and third-order nonlinear interactions.

Estimation of freak wave occurrence by the standard Boussinesq equation

In this section, first, the basic nonlinear properties using the standard Boussinesq equation were investigated through the comparison with the experimental data. Second, the probability density function of the maximum wave height as the freak wave occurrence was estimated using the simulated data through the nonlinear statistical wave properties. Here we will consider the strongest nonlinear case which corresponds to a JONSWAP-type spectrum with $\gamma_i = 10.0$ and wave steepness, H_i/L_p of 0.04 for the bathymetry Type 3 and Type 4.

Fig. 10 shows the spatial developments of the skewness and kurtosis for bathymetry Type 4. The notifications are same to Fig. 5, and the circles and squares are the experimental and simulated data, respectively. The vertical dashed bar indicates the line of $k_p h = 1.363$. The spatial development of the skewness as shown in the experimental results, which depends on the wave steepness following the second-order nonlinear theory given by Eq. 12 (Longuet-Higgins, 1963), cannot be seen in the simulated data of $k_p h > 1.363$ ($x/L_p < 10.76$). The nonlinear interactions given by the standard Boussinesq equation are expressed by the balance of the nonlinear term of $O(\epsilon)$ and the dispersion term of $O(\mu^2)$. However, although the simulated skewness are slightly increased by wave shoaling under the effect of the slope bottom when $k_p h$ becomes smaller than 1.363 ($x/L_p > 10.76$), they remain less than

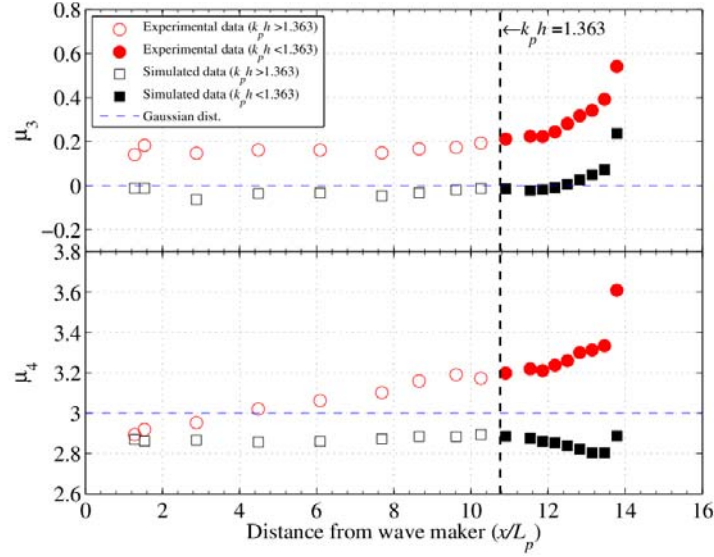


Figure 10. Spatial developments of skewness and kurtosis simulated by the standard Boussinesq equation for the bathymetry Type 4

one fifth of the experimental data. On the other hand, the simulated kurtosis of $k_p h > 1.363$ cannot show the spatial developments of the experimental data appropriately. The kurtosis evolutions caused by the quasi-resonant four-wave interactions at the order of $O(\epsilon^3)$ as shown in the experimental results but such high-order nonlinear interactions of more than $O(\epsilon, \mu^2)$ are not considered in the standard Boussinesq equation. Even in the shallow water regions of $k_p h < 1.363$ ($x/L_p > 10.76$), the numerical simulations significantly underestimate the nonlinear properties related to the freak wave occurrence. Thus, these results imply that the standard Boussinesq equation may not appropriately evaluate the freak wave occurrence caused by the quasi-resonant four-wave interactions from deep to shallow water regions. Therefore, it is necessary to correct the insufficient nonlinearity of the numerical simulations to describe the freak wave occurrence in the shallow water regions.

As mentioned above, we have investigated the significant differences of the nonlinear properties such as the development processes of the skewness and kurtosis between the numerical simulations and physical experiments. Therefore, we cannot evaluate the freak wave occurrence correctly in the shallow water regions using the simulated data unless solving the above mentioned insufficient nonlinearity. The nonlinearity of more than $O(\epsilon^2)$ which cannot be expressed in the standard Boussinesq equation is going to be corrected analytically. First, the corrected skewness μ_3' was given by Eqs. 12 and 14 considering the difference between the data of the numerical simulations and experiments in the deep water regions of $k_p h > 1.363$.

$$\mu_3' = \mu_3^{(2)} + \mu_3^{cal} \quad (14)$$

where μ_3^{cal} is the skewness given by the standard Boussinesq equation. $\mu_3^{(2)}$ is the skewness expressed by the second-order nonlinear theory of Longuet-Higgins (1963).

Next, the correction of kurtosis in the deep water regions of $k_p h > 1.363$ was conducted by using the spatial development process under the effects of the third-order nonlinear interactions from the experimental data, because there is no analysis solution for the kurtosis evolution in the deep water regions of $k_p h > 1.363$. The Eq. 15 was simply introduced by the spatial development of kurtosis in the deep water regions from the experimental data for the incident wave condition of $\gamma_i = 10.0$ and $H_i/L_p = 0.04$.

$$\mu_4^{(3)} = (\mu_4^{cal})_0 + 0.0184(x/L_p - 1.27) \quad (15)$$

where $\mu_4^{(3)}$ and $(\mu_4^{cal})_0$ are the corrected kurtosis in the deep water regions of $k_p h > 1.363$ and the kurtosis given immediately after wave generation, respectively. The second term of the right side of Eq.15 indicates the spatial development of kurtosis in the deep water regions for the experimental results. Following the above mentioned developments of the skewness and kurtosis given by Eqs. 14 and 15, the corrected kurtosis in the shallow water regions of $k_p h < 1.363$, μ_4' can be estimated by

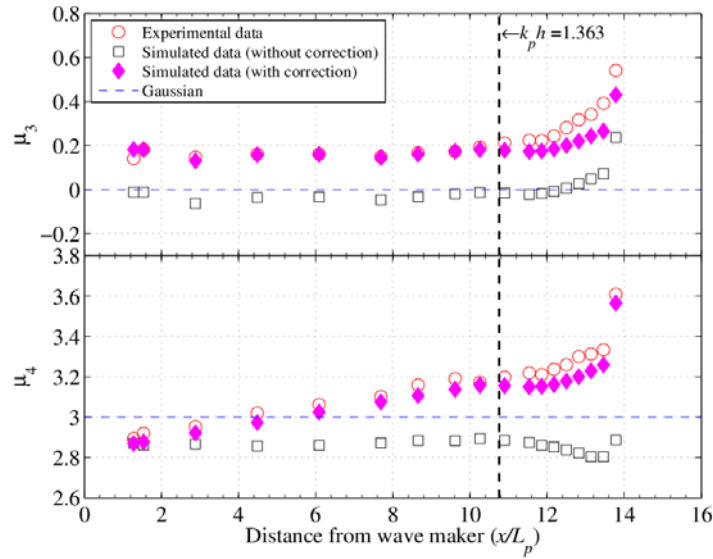


Figure 11. Spatial developments of skewness and kurtosis after analytical correction of the nonlinearity properties for the bathymetry Type 4

using the relational expression between the skewness and kurtosis (*i.e.*, Mori and Kobayashi, 1998). In our correction, the relational expression by Mori and Kobayashi (1998) is adopted, which is approximated by the Gaussian combination of the Stokes waves in the shallow water regions;

$$\mu_4' = \mu_4^{(3)} + \left(\frac{4}{3}\mu_3'\right)^2 \quad (16)$$

Fig. 11 shows the spatial developments of the skewness and kurtosis for the same condition in Fig. 10 by the above correction method. The filled diamonds are the simulated data corrected by Eqs. 14 to 16. Although there is a slight difference between the simulated data with the analytical correction and experimental data, the simulated data with the correction seems to describe a good agreement with the results of the experiments. Therefore, the behaviors of both skewness and kurtosis related to the freak wave occurrence in the shallow water regions can be estimated by the analytical correction of the insufficient nonlinearity of more than $O(\epsilon^2)$ to the standard Boussinesq equation, approximately.

Finally, in order to propose the estimation method of the freak wave occurrence, Fig. 12 shows the probability density function of the maximum wave height estimated by the analytical correction of the insufficient nonlinearity to the standard Boussinesq equation for the bathymetry Type 4. The probability density function of the maximum wave height was obtained by substituting the corrected kurtosis for MJ2006 as shown in Eq. 2. In MJ2006, the number of waves for one wave train was defined as $N = 200$. The solid line and the dashed line with the squares are the experimental data and the simulated data without the correction, respectively. The dashed line indicates the simulated data corrected by the insufficient nonlinearity of the standard Boussinesq equation analytically. We can see that the probability of the maximum wave height estimated by the above correction agrees with the experimental data, qualitatively, although there is a slight difference between them in terms of their peak values of the distributions. The further additional nonlinear correction will be required to adjust them, perfectly. Therefore, it is possible to understand the freak wave occurrence in the shallow water regions using the results of the numerical simulations using the standard Boussinesq equation, if appropriate higher-order nonlinear correction is considered analytically.

CONCLUSION

In this study, a series of the physical experiments in a wave tank and numerical simulations using the standard Boussinesq equation installed with several bathymetries were conducted to estimate the freak wave occurrence from deep to shallow water regions for unidirectional random waves. First, in the physical experiments, the maximum wave height is increased with an increase in kurtosis by the third-order nonlinear interactions in deep water regions of the dimensionless water depth $k_p h > 1.363$.

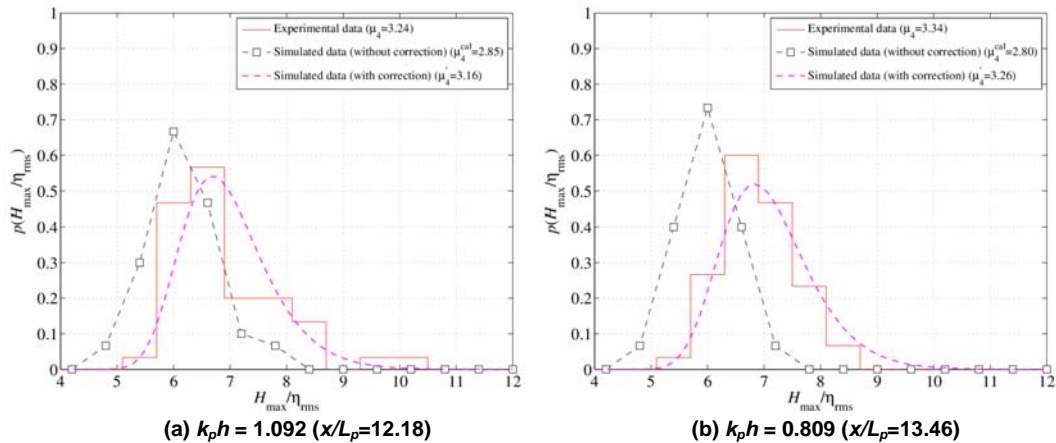


Figure 12. Probability density function of maximum wave height estimated by analytical correction for the bathymetry Type 4

The dependence of kurtosis on the freak wave occurrence is weakened under the effects of the second-order nonlinear interactions associated with wave shoaling in the intermediate to shallow water regions where $k_p h$ becomes smaller than 1.363. Moreover, it is possible to evaluate the freak wave occurrence from deep to shallow water regions by using the threshold value of $k_p h = 1.363$. Finally, although the standard Boussinesq equation cannot express the higher-order nonlinear interactions of more than $O(\varepsilon^2)$, it is possible to understand the freak wave occurrence in the shallow water regions by the analytical correction of the nonlinear properties (*i.e.*, development processes of skewness and kurtosis from deep to shallow water regions).

ACKNOWLEDGMENTS

We express our thanks to Professor Hajime Mase to give us fruitful advice for this research. This research was partially supported by the Ministry of Education, Science, Sports and Culture, Japan, though Grant-in-Aid (PI: Nobuhito Mori).

REFERENCES

- Hirayama, K., 2002. Utilization of numerical simulation on nonlinear irregular wave for port and harbor design. *Technical Note of The Port and Airport Research Institute*, No.1036, 162 (in Japanese).
- Hirayama, K., 2013a. Harbor tranquility analysis method for using Boussinesq-type nonlinear wave transformation model. *Proceedings of 23rd International Offshore and Polar Engineering Conference, Rhodes, Greece*.
- Hirayama, K., 2013b. Numerical simulations using Boussinesq model for random sea wave transformations. *11th International Workshop on Coastal Disaster Prevention*.
- Janssen, P.A.E.M., 2003. Nonlinear four-wave interactions and freak waves. *Journal of Physical Oceanography*, Vol.33 (4), 863-884.
- Janssen, P.A.E.M. and M. Onorato, 2007. The intermediate water depth limit of the Zakharov equation and consequences for wave prediction. *Journal of Physical Oceanography*, Vol.37 (10), 2389-2400.
- Longuet-Higgins, M., 1963. The effect on non-linearities on statistical distributions in the theory of sea waves. *Journal of Fluid Mechanics*, Vol.17, 459-480.
- Madsen, P.A. and O.R. Sørensen, 1992. A new form of the Boussinesq equations with improved linear dispersion characteristics. Part2. A slowly-varying bathymetry. *Coastal Engineering*, Vol.18, 183-204.
- Mori, N. and N. Kobayashi, 1998. Nonlinear distribution of nearshore free surface and velocity. *Proceedings of 26th International Conference of Coastal Engineering*, Vol.1, 189-202.
- Mori, N. and P.A.E.M. Janssen, 2006. On kurtosis and occurrence probability of freak waves. *Journal of Physical Oceanography*, Vol.36 (7), 1471-1483.

- Mori, N., M. Onorato, P.A.E.M. Janssen, A.R. Osborne and M. Serio, 2007. On the extreme statistics of long-crested deep water waves: Theory and experiments. *Journal of Geophysical Research*, 112, C09011, doi:10.1029/2006JC004024.
- Mori, N., M. Onorato and P.A.E.M. Janssen, 2008. Directional effects on freak wave prediction. *Proceedings of 31st International Conference of Coastal Engineering*, Vol.1, 392-403.
- Mori, N., M. Onorato and P.A.E.M. Janssen, 2011. On the estimation of the kurtosis in directional sea states for freak wave forecasting. *Journal of Physical Oceanography*, Vol.41 (8), 1484-1497.
- Mori, N. and T. Yasuda, 2001. Effects of high order nonlinear wave-wave interactions on random waves, *Proceeding of Rogue Waves 2000*, 229-244.
- Ochi, M. and W.C. Wang, 1984. Non-Gaussian characteristics of coastal waves. *Proceedings of 19th International Conference of Coastal Engineering*, Vol.1, 516-531.
- Petrova, P., and C. Guedes Soares, 2008. Maximum wave crest and height statistics of irregular and abnormal waves in an offshore basin, *Applied Ocean Research*, Vol. 30, 144-152.
- Trulsen, K., H. Zeng and O. Gramstad, 2012. Laboratory evidence of freak waves provoked by non-uniform bathymetry. *Physics of Fluids*, Vol.24, 097101.
- Waseda, T., T. Kinoshita, and H. Tamura, 2009. Evolution of a random directional wave and freak wave occurrence. *Journal of Physical Oceanography*, Vol.39, 621-639.
- Yasuda, T. and N. Mori, 1993. High order nonlinear effects on deep-water random wave trains. *International Symposium: Waves-Physical and Numerical Modelling, Vancouver*, Vol.2, 823-832.
- Yuen, H. and B.M. Lake, 1982. Nonlinear dynamics of deep-water gravity waves. *Advances in Applied Mechanics*, Vol.22, 67-327.
- Zeng, H and K. Trulsen, 2012. Evolution of skewness and kurtosis of weakly nonlinear unidirectional waves over a sloping bottom. *Natural Hazards and Earth System Sciences*, Vol.12, 631-638.